Available online at www.sciencedirect.com
ScienceDirect
Journal of Solid State Chemistry 181 (2008) 700–704
JOURNAL OF SOLID STATE CHEMISTRY
www.elsevier.com/locate/jssc

Determination of A-site deficiency in lanthanum manganite by XRD intensity ratio

Yanbo Zuo, Jianheng Li, Jianxin Yi, Zhongbing Wang, Chusheng Chen*

Laboratory of Advanced Functional Materials and Devices, Department of Materials Science and Engineering, University of Science and Technology of China, Hefei, Anhui 230026, P.R. China

Received 22 September 2007; received in revised form 12 December 2007; accepted 30 December 2007
Available online 6 January 2008

Abstract

A method based on the X-ray diffraction intensity ratio was developed to determine the maximum deficiency that the perovskite-structured $La_{1-x}MnO_{3\pm\delta}$ can accommodate at the A-site. Computer simulation predicts that the intensity ratio of (024) and (012) reflections for $La_{1-x}MnO_{3\pm\delta}$ in hexagonal setting increases with increasing the La deficiency x. XRD analysis shows that with increasing x until 0.09, the ratio increases as predicted, then levels off with further increase in x. An abrupt change in electrical conductivity is also observed at x of ~0.10. It is concluded that the maximum deficiency lies in between 0.09 and 0.10 for $La_{1-x}MnO_{3\pm\delta}$. The methodology presented in this paper in principle can be applied to other perovskite-structured materials.

Keywords: Lanthanum manganite; Intensity ratio; A-site deficiency; Electrical conductivity

1. Introduction

Lanthanum manganite of ABO_3 perovskite structure has been investigated extensively owing to its peculiar magnetoresistance properties and potential application in solid oxide fuel cells (SOFC) as cathodes [1–6]. The properties of the material are usually tailored by substitution of lanthanum with other elements such as Ca, Sr, and Ba. The properties can also be tuned by removing portion of cations from the A-site. The as-formed A-site deficient material exhibits a decreased electrical resistivity in the low-temperature range [4,7] and an increased ferromagnetic transition temperature (Curie temperature) [8]. And the chemical stability and inertness of the A-site deficient material is improved when it is used as cathode material in SOFC [9].

There have been some studies on the maximum deficiency that the lanthanum manganite lattice can accommodate at the A-site, but reported results are confusing. van Roosmalen et al. reported a value of 0.09 for $La_{1-x}MnO_3$ in the temperature range of 1000–2000 K, beyond which a second phase Mn_3O_4 appears [9]. A higher value of 0.11–0.13 was reported [8,10] and an even higher value of 0.30 was reported by Gupta et al. [5]. The discrepancy in the reported maximum deficiency may arise partly from the different sample preparation routes used, and/or the different characterization methods adopted. A convenient method to determine the maximum deficiency is to detect the first appearance of Mn_3O_4 in the $La_{1-x}MnO_3$ sample. But, this method often gives a higher maximum deficiency than the real one, because the amount of the second phase at its first appearance may be below the detection limit. Direct determination of the deficiency is possible with neutron diffraction [11], but this method also has its limitation due to the accessibility of the neutron diffraction facility. In this paper, we propose an alternative and simpler method to determine the maximum deficiency, in which the intensity ratio of XRD reflections (024) and (012) for $La_{1-x}MnO_{3\pm\delta}$ in hexagonal setting is examined as a function of the lanthanum content in the material.

2. Theory and computer simulation

The intensity of a reflection is known to be determined by the incident X-ray intensity, the composition, structure

*Corresponding author. Fax: +86 551 3601592.
E-mail address: ccsm@ustc.edu.cn (C. Chen).

0022-4596/$ - see front matter © 2008 Elsevier Inc. All rights reserved.
doi:10.1016/j.jssc.2007.12.033

and status of specimen and the operation parameters of the diffractometer. The intensity of (hkl) reflection, I_{hkl} from powder specimens is described by

$$I_{hkl} = KI_0VJ_{hkl}(\mathrm{LP})_{hkl}F^2_{hkl}e^{-2M}A^{-1}(\theta), \quad (1)$$

where K is a constant, I_0 the incident X-ray intensity, V the volume of diffraction powder, J_{hkl} the multiplicity factor, $(\mathrm{LP})_{hkl}$ the Lorentz-polarization factor, F_{hkl} the structure factor, e^{-2M} the temperature factor, and $A(\theta)$ the absorption factor.

Crystalline oxides of ABO_3 structure can be considered as the stacking of two sets of mutually interpenetrating lattice planes AO and BO_2. And scattering of X-rays from these two planes gives rise to reflections indexed by (024) and (012) in hexagonal setting, corresponding to (002) and (001) in cubic setting, respectively. Reflection (024) is more intense than reflection (012), because the former arises from the constructive interference of waves scattered from AO with those from BO_2 whereas the latter the destructive interference. Obviously, changes in the occupancy of the cations on AO lattice planes should be manifested by the changes of the intensities of the two reflections. In practice, it is more appropriate to characterize the changes in the cation occupancies by using the intensity ratio of the two reflections rather than the intensity, for the intensity ratio will not be affected by the preferred orientation of the sample. The errors in the measurement of the intensity are cancelled because (012) and (024) are different orders of the same reflecting plane.

A computer simulation was conducted to examine how the change in the A-site deficiency affects the intensity ratio of reflections (024) and (012) for $La_{1-x}MnO_3$ with x varying from 0.0 to 0.10. The intensity ratio was calculated using program POWDERCELL [12]. Since the oxide may exhibit oxygen nonstoichiometry [3,9], calculation was also performed to examine its effect on the intensity ratio and compare with the A-site deficient sample. Parameters used for simulation were given as follows: Bragg-Branteno geometry, radiation Cu$K\alpha_1$; space group $R\bar{3}c$, $a=b=5.5263$ Å, $c=13.356$ Å; lanthanum ion site position (0, 0, 0.25) in 6a, site occupation factor (SOF) = 1.000–0.900; manganese ion (0, 0, 0) in 6b, SOF = 1.000–0.909; oxide ion (0.5503, 0, 0.25) in 18e, SOF = 1.000–0.900 [13].

3. Experimental

Lanthanum manganites powders of nominal composition $La_{1-x}MnO_{3\pm\delta}$ ($x = 0$, 0.05, 0.08, 0.09, 0.10, 0.12, 0.15) were synthesized via a citrate route. Appropriate amount of La_2O_3 that had been calcined at 1000 °C was dissolved in nitric acid and mixed with $Mn(NO_3)_2$ solution, then citric acid was added according to the molar ratio of citric acid and metal ions 3:2. The as-obtained solution was adjusted to a pH of 7, evaporated at 80 °C to yield light yellow gels. The gels were burned in air, followed by calcination at 1100 °C for 10 h in air. The as-prepared powders were isostatically pressed into bars under 300 MPa pressure, sintered in air at 1250 °C for 15 h, and cooled to room temperature at a rate of 2 °C/min.

The La/Mn ratio of $La_{1-x}MnO_{3\pm\delta}$ powders was determined by induced coupled plasma spectroscopy (ICP, Atomscan Advantage). XRD was performed using Philips X′Pert Pro diffractometer with Cu$K\alpha$ radiation in the Bragg–Branteno geometry. The powder used for analysis was sieved with 250 mesh. The X-ray tube voltage was set at 40 kV and current 30 mA. Continuous scan mode was used with a scanning rate of 4°/min and scanning range from 20 to 80°, and the collected diffraction data were treated involving background deduction, $K\alpha_2$ stripping and profile fitting with program HIGHSCORE.

The electrical conductivity of a whole series of samples $La_{1-x}MnO_{3\pm\delta}$ with x ranging from 0 to 0.15 was measured at elevated temperatures in air with an electrochemical station CHI604B using a DC four-probe electrode setting.

4. Results and discussion

The La/Mn ratio of $La_{1-x}MnO_{3\pm\delta}$ ($0\leqslant x\leqslant 0.15$) determined by ICP is given in Table 1. It can be seen that the actual La/Mn ratio of the samples is very close to the nominal value. XRD analysis reveals that the samples of nominal composition $La_{1-x}MnO_{3\pm\delta}$ consist of a rhombohedral perovskite-structured oxide as the major phase (space group $R\bar{3}c$). And a spinel-structured Mn_3O_4 appears at $x\geqslant 0.12$ (see Fig. 1), indicating that the maximum A-site deficiency value cannot be greater than 0.12. The second phase Mn_3O_4 might have appeared at x less than 0.12, but its quantity may be well below the detection limit of the XRD method, thus the precise value for the maximum deficiency needs to be determined by other methods.

Fig. 2 shows the calculated intensity ratio of reflections (024) and (012) for $La_{1-x}MnO_3$. It can be seen clearly that the intensity ratio increases with increasing A-site deficiency x. With x increasing from 0 to 0.10, the intensity ratio increases by 47% from 2.16 to 3.18. The lanthanum manganite normally exhibits oxygen nonstoichiometry as represented by formula $LaMnO_{3\pm\delta}$. The effect of oxygen nonstoichiometry on the intensity ratio is also accessed by computer simulation, and the results are presented in Fig. 3. Since the perovskite-structured oxide cannot contain excessive oxygen at interstitial positions, the incorporation of excessive oxygen leads to the creation of

Table 1
La/Mn ratio of $La_{1-x}MnO_{3\pm\delta}$ determined by ICP

X	Nominal	Measured
0	1.00	1.008(8)
0.05	0.95	0.946(8)
0.08	0.92	0.922(8)
0.09	0.91	0.906(8)
0.10	0.90	0.903(8)
0.12	0.88	0.886(8)
0.15	0.85	0.855(8)

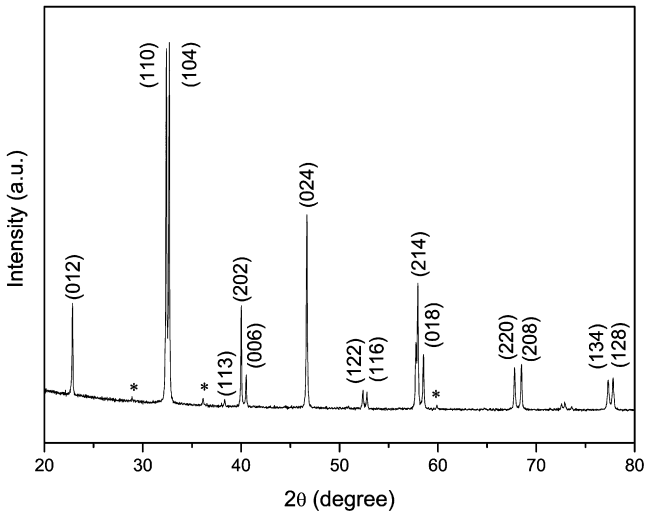

Fig. 1. XRD pattern of $La_{0.85}MnO_{3-\delta}$, indexed as $R\bar{3}c$ space group (hexagonal setting); reflections of Mn_3O_4 are marked with asterisks.

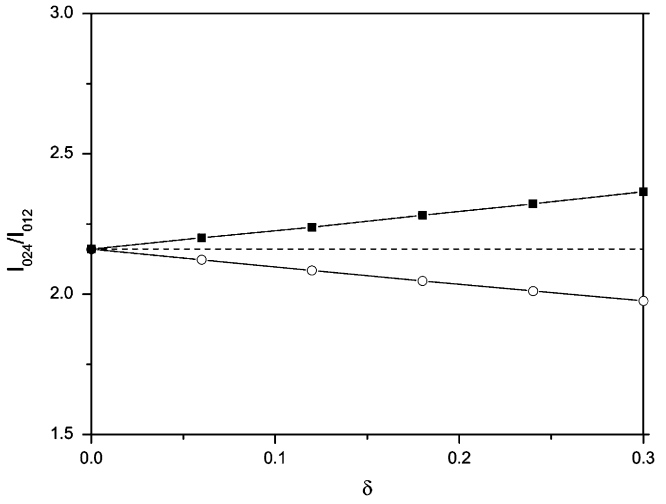

Fig. 3. Calculated intensity ratio I_{024}/I_{012} as a function of oxygen nonstoichiometry in $LaMnO_{3\pm\delta}$. (■) oxygen excess, (○) oxygen deficient. Dotted line is guided to the eye.

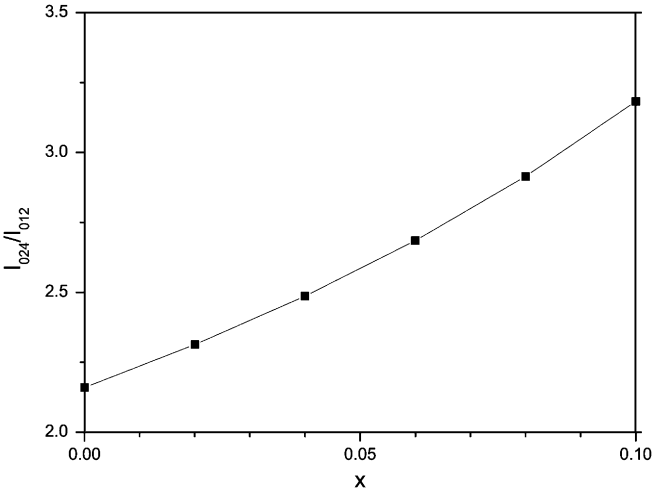

Fig. 2. Calculated intensity ratio of the (024) and (012) reflections as a function of La deficiency x in $La_{1-x}MnO_3$.

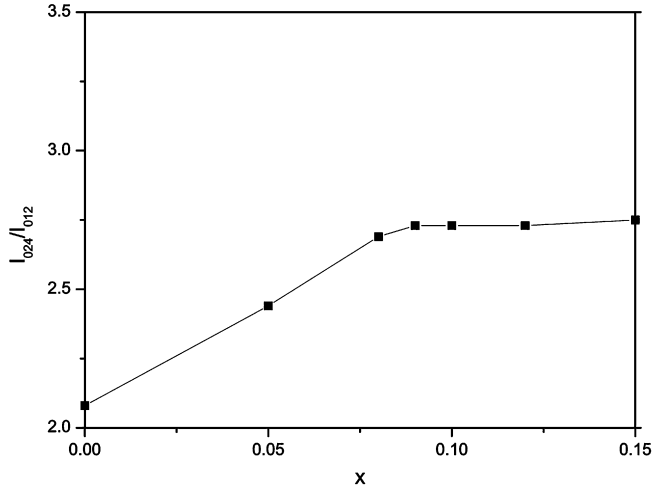

Fig. 4. Measured intensity ratio I_{024}/I_{012} as a function of La deficiency x in $La_{1-x}MnO_{3\pm\delta}$.

cation vacancies at both A and B sites [14,15]. Thus, oxygen-excessive $LaMnO_{3+\delta}$ is more appropriately represented by the formula $La_{1-y}Mn_{1-y}O_3$ with $y=\delta/(3+\delta)$, and simulation was done with this defect chemistry model. From Fig. 3, it can be seen that the intensity ratio increases with increasing the oxygen excess δ, but this increase is much smaller than that for $La_{1-x}MnO_3$. As to the oxygen-deficient $LaMnO_{3-\delta}$, the intensity ratio is decreased with increasing oxygen vacancies. At oxygen deficiency δ of 0.3, i.e., the site occupation for oxide ion in the lattice is 90%, the intensity ratio is decreased by ~9%.

The XRD intensity ratio for $La_{1-x}MnO_{3\pm\delta}$ was measured, and compared with the results of the above-described computer simulation. Fig. 4 shows that the measured intensity ratio increases with increasing x until $x\approx0.09$; the intensity ratio is increased by 31% from 2.08 at $x=0.00$ to 2.73 at $x=0.09$. By comparing the measured results with the computer simulation (Figs. 2 and 3), it becomes clear that the observed increase in the intensity ratio for $La_{1-x}MnO_3$ can be attributed to the presence of vacancies at the A-site. Fig. 4 also shows that for samples with x larger than ~0.09, the intensity ratio levels off. This reveals that the maximum A-site deficiency for $La_{1-x}MnO_{3\pm\delta}$ lies at ~0.09. Beyond that value, the material enters the two-phase region of A-site deficient perovskite oxide and Mn_3O_4; in other words, the phase boundary is located at x of ~0.09. In the two-phase region, the content ratio of the two phases varies with x, but the chemical composition and crystal structure of each phase remain unchanged with the variation of x, thus the intensity ratio of the perovskite phase keeps constant in this composition region.

In practice, the phase boundary is often judged from the variation of the lattice parameters with composition [2,9].

From Fig. 5, one can see that the lattice parameters fluctuate with x. Apparently, it is impossible to determine the phase boundary and thus the maximum A site deficiency from Fig. 5. One possible reason for the failure is that the A-site deficiency is not the only factor affecting the lattice parameters of the perovskite phase. The lattice parameters are also affected by the oxygen nonstoichiometry δ [16,17], which in turn is very dependent on the preparation conditions [18]. As a matter of fact, it is difficult to ensure that all the samples are prepared under the same conditions and have same degree of oxygen nonstoichiometry.

The electrical conductivities of $La_{1-x}MnO_{3\pm\delta}$ were measured at elevated temperatures of 700–1000 °C in air. As can be seen from Fig. 6, an abnormal change occurs at x of ~0.10. This is a sign that the perovskite phase has reached a maximum deficiency at A-site. The observed increase in the conductivity with increasing x at $x<0.10$ is consistent with the results given in the literature [1,5,7]. It is known that the material is a p-type conductor [19], and the introduction of vacancies at A site leads to a higher concentration of Mn^{4+} ions (electron holes) at B site [2,20]. The decreased electrical conductivity at $x>0.10$ is likely due to the appearance of the second phase Mn_3O_4 which is a poor electronic conductor and thus blocks the transport path of electrons along the perovskite phase [21].

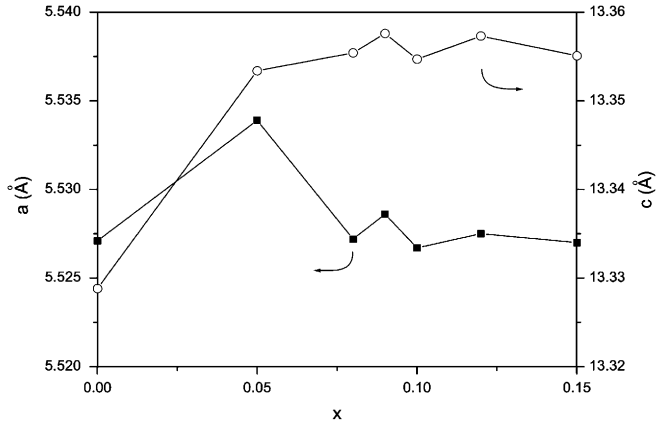

Fig. 5. Measured lattice parameters a and c as a function of La deficiency x in $La_{1-x}MnO_{3\pm\delta}$.

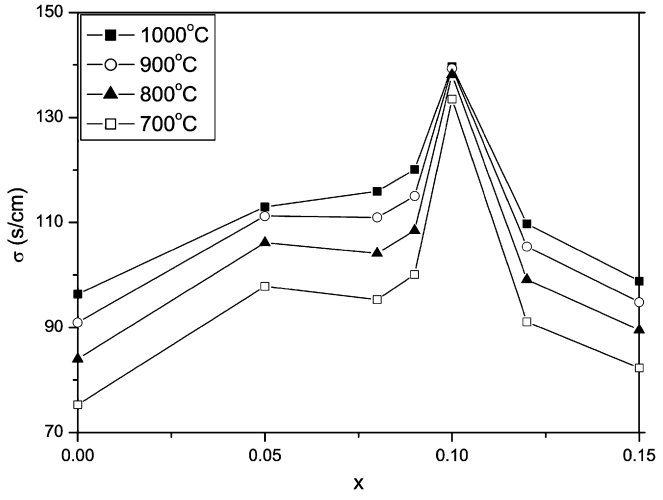

Fig. 6. Measured electrical conductivity σ at various temperatures as a function of La deficiency x in $La_{1-x}MnO_{3\pm\delta}$.

5. Conclusions

The A-site deficiency in perovskite-structured $La_{1-x}MnO_{3\pm\delta}$ has been analyzed using the XRD intensity ratio method. Computer simulation reveals that the intensity ratio I_{024}/I_{012} for $La_{1-x}MnO_3$ increases significantly with increasing lanthanum deficiency x at the A site. XRD analysis shows that the intensity ratio increases with x until $x=0.09$, beyond which it levels off. The electrical conductivity also shows an abrupt change at x of 0.10. From these studies, it is concluded that the A-site maximum deficiency lies at 0.09–0.10 for $La_{1-x}MnO_{3\pm\delta}$. The intensity ratio method proposed in this study in principle can be applied to other perovskite-structured materials especially in combination with measurements of electrical conductivity and other physical properties.

Acknowledgment

This work was supported by National Science Foundation of China (Grant no.: 50332040).

References

[1] J.A.M. van Roosmalen, J.P.P. Huijsmans, L. Plomp, Solid State Ionics 66 (1993) 279–284.
[2] J. Töpfer, J.B. Goodenough, Chem. Mater. 9 (1997) 1467–1474.
[3] G. Dezanneau, A. Sin, H. Roussel, M. Audier, H. Vincent, J. Solid State Chem. 173 (2003) 216–226.
[4] S. de Brion, F. Ciorcas, G. Chouteau, P. Lejay, P. Radaelli, C. Chaillout, Phys. Rev. B59 (1999) 1304–1310.
[5] A. Gupta, T.R. McGuire, P.R. Duncombe, M. Rupp, J.Z. Sun, W.J. Gallagher, G. Xiao, Appl. Phys. Lett. 67 (1995) 3494–3496.
[6] J. Nowotny, M. Rekas, J. Am. Ceram. Soc. 81 (1998) 67–80.
[7] G.J. Chen, Y.H. Chang, H.W. Hsu, Mater. Sci. Eng. B68 (1999) 104–110.
[8] P.A. Joy, C. Raj Sankar, S.K. Date, J. Phys.: Condens. Matter 14 (2002) L663–L669.
[9] J.A.M. Van Roosmalen, P. van Vlaanderen, E.H.P. Cordfunke, W.L. IJdo, D.J.W. IJdo, J. Solid State Chem. 114 (1995) 516–523.
[10] M. Palcut, K. Wiik, T. Grande, J. Phys. Chem. C111 (2007) 813–822.
[11] M. Wolcyrz, R. Horyń, F. Bourée, E. Bukowska, J. Alloys Compd. 353 (2003) 170–174.
[12] G. Nolze, W. Kraus, Powder Diffr. 13 (1998) 256–259.
[13] A.K. Cheetham, C.N.R. Rao, T. Vogt, J. Solid State Chem. 126 (1996) 337–341.
[14] J.A.M. Van Roosmalen, E.H.P. Cordfunke, J. Solid State Chem. 110 (1994) 106–108.
[15] K. Nakamura, K. Ogawa, J. Solid State Chem. 163 (2002) 65–76.
[16] S. Miyoshi, A. Kaimai, H. Matsumoto, K. Yashiro, Y. Nigara, T. Kawada, J. Mizusaki, Solid State Ionics 175 (2004) 383–386.
[17] J.A. Alonso, M.J. Martínez-Lope, M.T. Casais, J.L. MacManus-Driscoll, P.S.I.P.N. de Silva, L.F. Cohen, M.T. Fernández-Díaz, J. Mater. Chem. 7 (1997) 2139–2144.

[18] G. Dezanneau, M. Audier, H. Vincent, C. Meneghini, E. Djurado, Phys. Rev. B69 (2004) 014412.
[19] J. Mizusaki, Y. Yonemura, H. Kamata, K. Ohyama, N. Mori, H. Takai, H. Tagawa, M. Dokiya, K. Naraya, T. Sasamoto, H. Inaba, T. Hashimoto, Solid State Ionics 132 (2000) 167–180.
[20] S.J. Kim, C.S. Kim, S. Park, B.W. Lee, J. Appl. Phys. 89 (2001) 7416–7418.
[21] M. Mori, N.M. Sammes, E. Suda, Y. Takeda, Solid State Ionics 164 (2003) 1–15.